Flow through doubly connected ducts

S. C. Solanki*, J. S. Saini† and C. P. Gupta‡

Fluid flow in doubly connected ducts, bounded externally by a circle and internally by a regular polygon of various shapes, is analysed using the finite element method. Hydrodynamically developed, steady, laminar flow of a constant-property fluid is considered. Velocity profiles as well as friction factors (at the inner and outer walls, and average value) are presented. These compare well to previous results available in the literature. Salient characteristics of flow are identified. Correlations for the average friction factor with aspect ratio are suggested.

Keywords: *doubly connected ducts, hydrodynamically developed flow, friction factor, aspect ratio, Reynolds number*

Introduction

Non-circular ducts are widely used in compact heat exchangers, regenerators for waste heat recovery, extrusion ducts of polymer processing plants, and heat exchangers employed in food-processing industries. They are also encountered in rod-cluster assemblies in nuclear reactors and in supply passages for bearings. Although several investigators[1,2] have studied the fluid flow and heat transfer characteristics of non-circular ducts, it appears that very little is known about the mechanism of fluid flow and heat transfer through non-circular annular passages which find applications, for example, in shipping casks which are used to passively cool the spent reactor fuel subassemblies[3,4].

An excellent survey of laminar-flow forced convection in ducts has been presented by Shah and London[2], in which doubly connected duct geometries are also covered. The Schwarz–Neumann alternating method (an approximate method of conformal mapping)[5], the Gram–Schmidt ortho-normalization technique[6], the collocation method[7] and the least square approximation method[8] have been employed to obtain the solution for doubly connected ducts bounded externally by a circle and internally by a polygon. The finite difference method has been used successfully to tackle complex duct geometries[9,10]. Experimental results are reported in Ref 11 for four annular passages consisting of an outer circular tube and an inner core of one of the following cross-sections: (i) equilateral triangle, (ii) right isosceles triangle, (iii) square, and (iv) rectangle of aspect ratio 1.66. The range of Reynolds number (based on hydraulic diameter) was from 5000 to 20 000. In Ref 12 an experimental investigation of fully developed laminar flow in a non-circular annulus bounded by a circle on the outside and a square on the inside is presented.

In the present paper the results of an analysis of laminar flow in non-circular annular passages bounded externally by a circular tube and internally by each one of the following cross-sections are reported: (i) equilateral triangle, (ii) square, (iii) regular hexagon, (iv) regular octagon, (v) 18-sided regular polygon. In addition, circular annuli are also considered for the purpose of testing the algorithm developed. A finite element solution algorithm has been developed for the two-dimensional equations for the motion of a constant-property Newtonian fluid in the laminar hydrodynamically developed regime under steady state conditions. It provides detailed information on the velocity field in addition to overall results of engineering interest. No difficulties such as negative velocity and negative shear stress values, as encountered by Cheng and Jamil[7], occur with the present method. Moreover, the present algorithm requires, for each case, about 5 s as CPU time on a DEC 20-50 computer system when the number of elements is taken as 145 (number of total nodes being 175) in the smallest symmetrical section of the duct. With just half the number of elements, consuming about half the time, results of accuracy comparable to those given in Refs 7 and 8 are obtained.

Governing equation

The annular passage in which flow takes place is shown in Fig 1. The inner core is concentric with the outer tube and has sharp corners. For the steady, laminar, fully developed flow of a Newtonian fluid with constant properties, the governing momentum equation in the dimensionless form in the cylindrical polar coordinate system is

$$\frac{\partial^2 u}{\partial R^2}+\frac{1}{R}\frac{\partial U}{\partial R}+\frac{1}{R^2}\frac{\partial^2 U}{\partial \theta^2}-1=0 \qquad (1)$$

The boundary condition associated with Eq (1) is

$$U=0;\ \text{no slip at both the boundaries} \qquad (2)$$

Method of solution

The finite element method (FEM) is adopted to obtain numerical solutions to Eq (1). The method of weighted

* Department of Mechanical Engineering, College of Technology, University of Aden, Maala, Aden, PDR Yemen
† Alternate Hydro Energy Centre, University of Roorkee, Roorkee–247667, India
‡ Department of Mechanical and Industrial Engineering, University of Roorkee, Roorkee–247667, India
Received 11 April 1985 and accepted for publication on 14 May 1986

residuals with the Galerkin criterion[13] is used to obtain the finite element equations corresponding to Eq (1). Linear variation of velocity within an element is assumed. The elements chosen are the two-dimensional linear isoparametric elements[13]—in particular, the elements formed by the cylindrical coordinates as shown in Fig 2.

The smallest symmetrical portion, area abcd, of the cross-section of fluid flow is subdivided into smaller elements in a manner shown in Fig 2. As seen from this figure, the elements formed are four-node curvilinear quadrilaterals. The radial line at the corner, cd, is divided into 10 parts, while all other radial lines have more divisions in order to reduce the size of the elements near the inner wall. The latter is achieved by taking a circular arc from each node on the inner wall (ad) to obtain 4-node curvilinear quadrilaterals. Some typical elements are marked by hatch lines. This kind of subdivision gave more elements near the inner non-circular boundary, on which a peripheral variation of quantity like shear stress is expected. The results for the non-circular annular

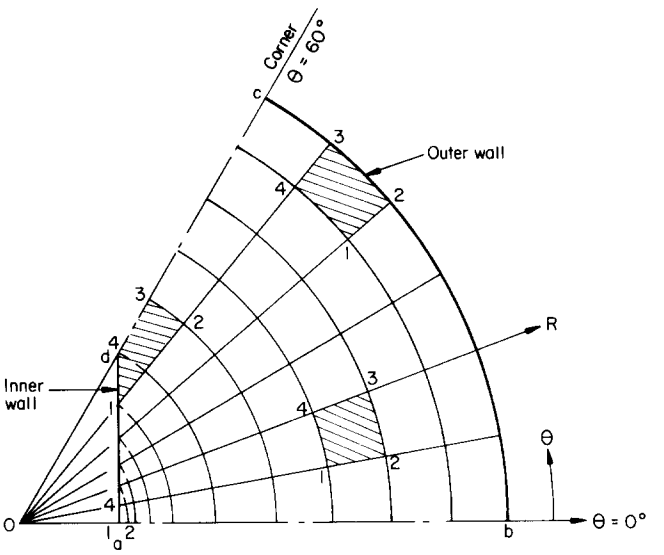

Fig 2 Elements: abcd is smallest symmetrical portion of the cross-section. Shaded subdomains are some typical elements. Total number of elements is 145; total number of nodes is 175

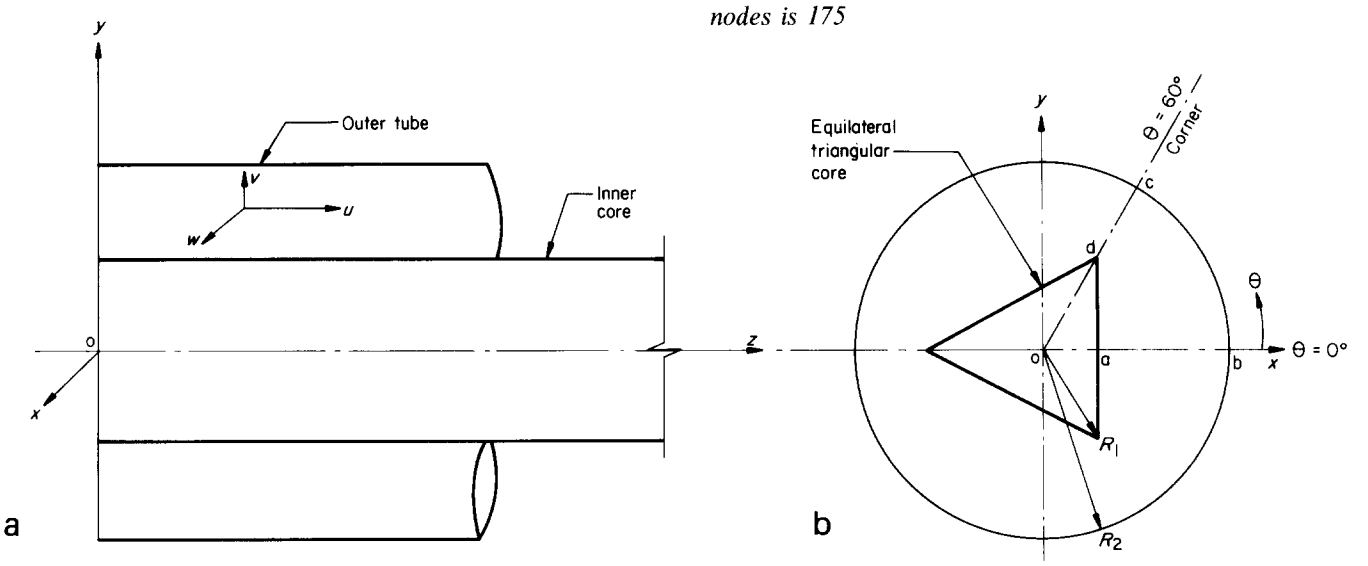

Fig 1 Coordinate system: (a) longitudinal section; (b) cross-section. The aspect ratio $\beta \equiv R_1 R_2$

Notation

A	Area of flow, m^2
C_1	Constant $\equiv (dp/dz)$, $m^{-1} s^{-1}$
D_h	Hydraulic diameter $\equiv 4A/P$, m
f	Friction factor $\equiv 2\tau_w/\bar{u}^2$ (dimensionless)
$f\,Re$	Product of friction factor and Reynolds number (dimensionless)
$(f\,Re)_1$	Value of $f\,Re$ at the inner wall (f is based on the circumferentially averaged shear stress at the inner wall)
$(f\,Re)_2$	Value of $f\,Re$ at the outer wall (f is based on the circumferentially averaged shear stress at the outer wall)
$\bar{f}\,Re$	Average $f\,Re$ (ie the product of the average friction factor and Reynolds number)
P	Wetted perimeter $\equiv P_1 + P_2$, m
P_1, P_2	Perimeters of the inner and outer boundaries, respectively, m
p	Pressure, N/m^2
r, θ, z	Polar coordinates: radial, m; angular, rad; axial, m
R	Radial distance $\equiv r/R_2$ (dimensionless)
R_1, R_2	Radii of the corner of the inner core and the outer circular tube, m
Re	Reynolds number $\equiv \rho\bar{u}D_h/\mu$ (dimensionless)
u	Velocity in axial (z) direction, m/s
U	Velocity $\equiv u/C_1R_2^2$ (dimensionless)
$\bar{u}$, $\bar{U}$	Average u and average U, respectively
β	Aspect ratio $\equiv R_1/R_2$ (dimensionless)
ρ	Density, kg/m^3
μ	Dynamic viscosity, kg/m s
τ_w	Wall shear stress, N/m^2

Subscripts

max	Maximum velocity point
1	Inner wall
2	Outer wall

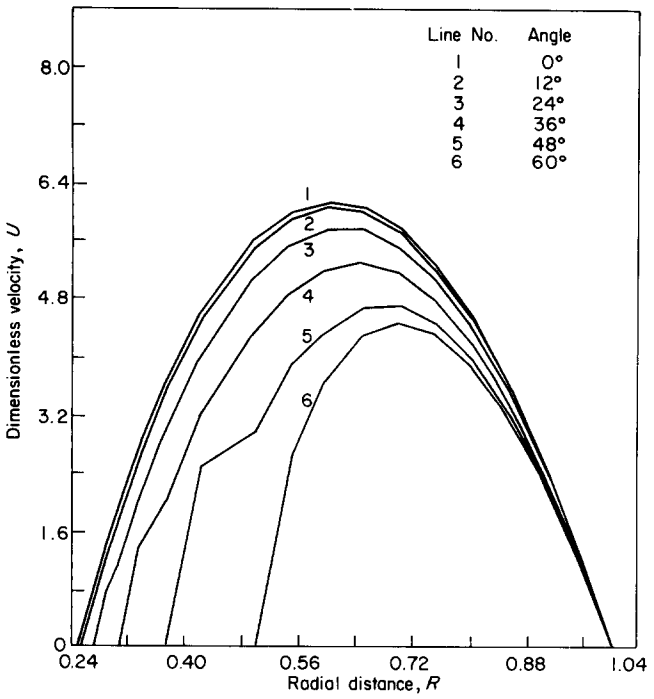

Fig 3 Velocity profiles for annulus with an equilateral triangular core, $\beta=0.5$. Number of elements is 145

passages given here are for the mesh grid having a total of 145 elements and 175 nodes. Smaller numbers of elements (from 22 to 145 elements) were also tried in order to apply a convergence test. The criterion for convergence was taken to be the overall result, ie the product of average friction factor and Reynolds number. A total of 145 elements was found to be adequate.

Results and discussion

The results which are presented here are the velocity profiles (Figs 3–6), the average friction factor, and the friction factors at the inner and outer walls (Figs 7–8).

Confirmatory results

Circular annulus case

The algorithm developed is tested with a circular annulus for which the exact solution is available[2]. The comparison of both the details (Fig 6) and overall results (Fig 8) is found to be excellent. For the sake of clarity, distinguishing points corresponding to the exact solution are not marked on Fig 8. The FEM solution overpredicts $\bar{f}\,Re$, $(f\,Re)_1$ and $(f\,Re)_2$ values—maximum deviation being of the order of one percent only.

Non-circular annuli

Comparison of the values of the product of the average friction factor and Reynolds number, $\bar{f}\,Re$, with previous results[2,8] shows good agreement, deviation ranging from one percent at the low aspect ratios to about ten percent at the high aspect ratios.

A high degree of similarity is also observed between the present velocity solution for the non-circular annulus for $\beta=0.999$ and that for the circular segment cross-section $(\beta-1)$ of 120° included angle between the radial lines forming the section[14], the latter being a limiting case for the type of non-circular annuli under consideration; maximum deviation is of the order of four percent.

The general characteristics of the flow field are identified and discussed in the following paragraphs.

Velocity field

Velocity profiles

Typical velocity profiles are shown in Figs 3–5. Similar trends of the velocity variations are found for the other non-circular annuli studied and for higher and lower aspect ratios in each case. Hence, figures for other cases are not given here.

It is observed, from the velocity plots, that for low aspect ratios, the velocity profiles do not vary with θ in most of the domain, except near the inner wall. The variation near the inner wall is attributed to non-symmetry of the inner wall with respect to θ. As the aspect ratio increases, the angular variation increases. This implies that the effect of the inner non-circular wall penetrates further towards the outer wall as the aspect ratio increases. In essence, this leads to a great simplification: that the velocity field in the fully developed region can be considered one-dimensional up to a certain aspect ratio dependant on the shape of the inner core as listed in Table 1.

Peak velocity and shear stress distribution

It is found that when the angular variation exists, the peak, U_{max}, of the velocity profile at a particular value of θ is highest at the section through the midpoint of the side of the inner core and is lowest at the section through its corner for all aspect ratios, for all annuli studied.

The values of U_{max} and those of U in general decrease with an increase in θ. In view of the common observation that more fluid tends to flow through the portion of lesser resistance, it may be concluded for the flow through the non-circular annular passages that the shear stresses in the region near and at the corner are more than those in the region near $\theta=0°$. This is substantiated by the plots of isovels (Fig 4) which show the distribution of shear stresses in the entire flow field if one observes relative distances between isovels. The shear stress in the region near the inner wall is larger than that in the region near the outer wall (Fig 4); the difference between the two becomes larger as the aspect ratio decreases. This is more clearly demonstrated in Fig 7, where it is seen that $(f\,Re)_1$ is considerably greater than $(f\,Re)_2$ for low aspect ratios. This is true with each case of the annuli studied.

Table 1 Maximum value of aspect ratio at which velocity field in fully developed region can be considered one-dimensional

No of inner core sides	3 and 4	6	8	18
Aspect ratio β	0.1	0.3	0.5	0.7

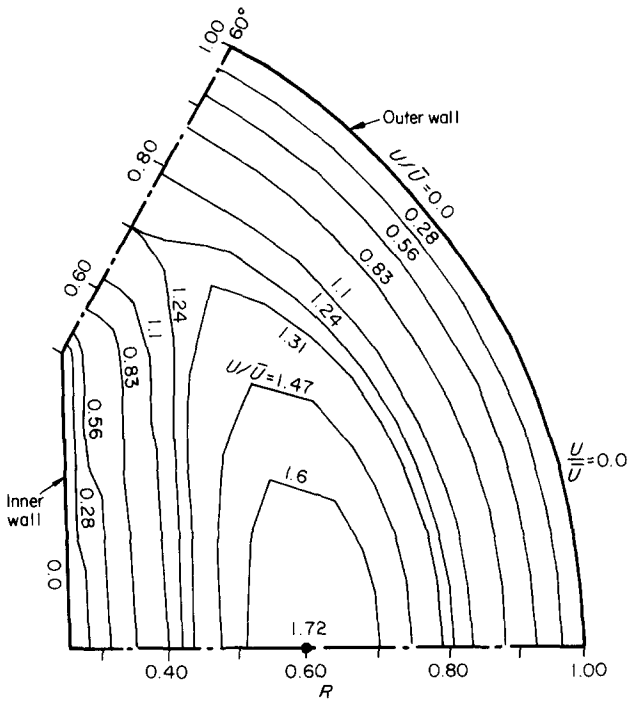

Fig 4 Isovels for annulus with an equilateral triangular core, $\beta = 0.5$

Skewness of the velocity profiles

Another effect of unequal distribution of shear stresses on the inner and outer walls is reflected in the skewness of the velocity profiles, ie the shift of the location of the peak velocity towards the inner wall. Such a shift is observed in the case of a circular annulus too, but in the case of non-circular annuli it is a function of θ. Non-symmetry of the boundary walls with θ results in dependence on θ. The shift, for both the circular and the non-circular annuli, depends on aspect ratio: for lower aspect ratios the shift towards the inner wall is greater because the predominance of the shear stresses at the inner wall over those at the outer wall is greater for low aspect ratios.

Effect of the number of core sides

The velocity plots reveal that the angular variation of velocity gradually reduces as n, the number of sides of the regular polygonal core, increases from 3 to 18; negligible angular variation of velocity exists when $n = 18$ for most of the range of aspect ratio values (see Fig 6). It can be related to the sharpness of a corner of the inner core, which decreases as n increases.

Comparison with the flow field in a circular annulus

A point worth examining at this juncture is how closely the flow field in a non-circular annulus compares with that in a circular annulus. Since no angular variation is observed for the non-circular annuli with an 18-sided core, the velocity profiles for this case are compared with those of circular annuli (Fig 6). As seen there, the velocity profiles for the two annuli coincide for most of the range of aspect ratio. Only at higher aspect ratios is a deviation observed. For example, when aspect ratio is 0.9, the peak velocity and the velocities in the region close to it are overpredicted by the circular annulus profile by about 7%.

As shown in Fig 8, the overall quantities of engineering interest, namely friction factors, can be predicted very closely (within ± 1.6 percent) for the annuli with an 18-sided core for aspect ratio varying from 0.02 to 0.9 from the circular annulus results, which are well known. The deviation is large for aspect ratio greater than 0.9. This is expected also, since the limiting cases when aspect ratio approaches 1 for the two annuli are different; the limiting case for the circular annulus is a parallel-plate configuration and that for the non-circular annulus under consideration is a circular segment duct.

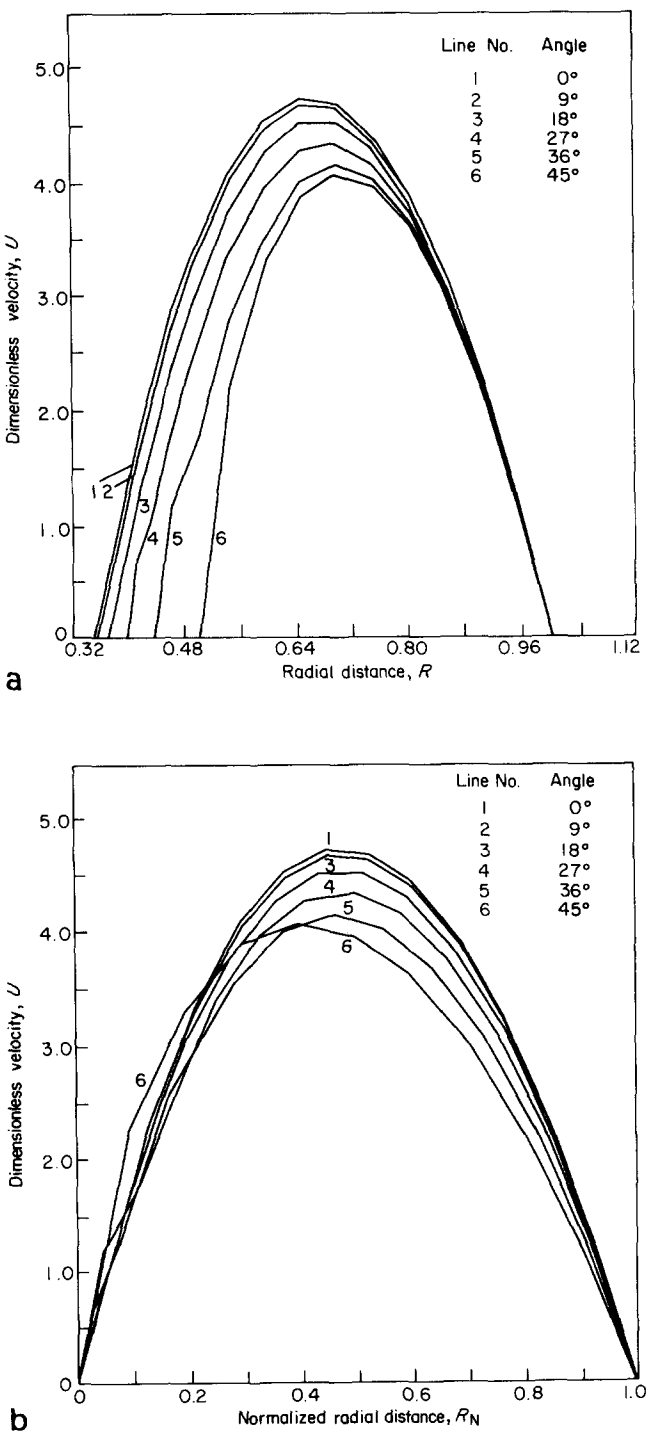

Fig 5 Velocity profiles for annulus with a square core, $\beta = 0.5$: (a) U versus R; (b) U versus R_N. Number of elements is 145

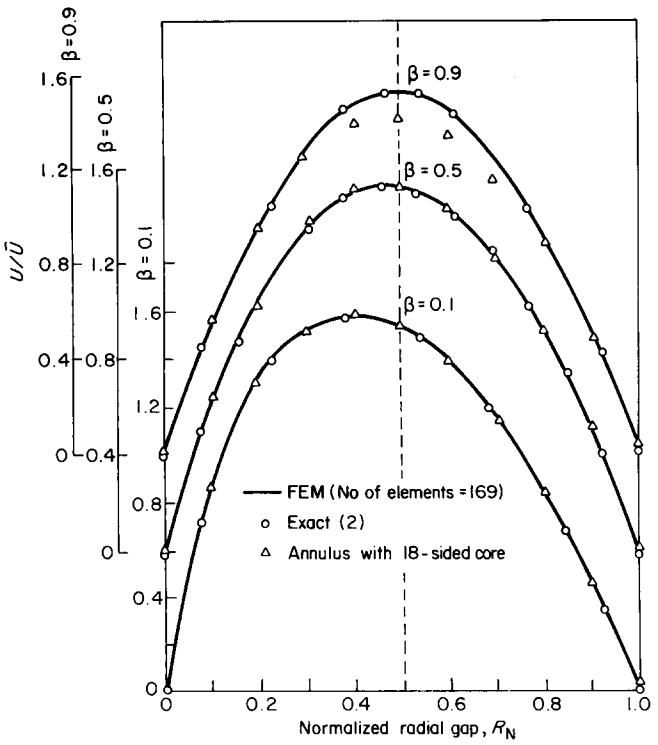

Fig 6 Velocity profiles for circular annuli and annuli with an 18-sided core, $\beta = 0.1$, 0.5, and 0.9

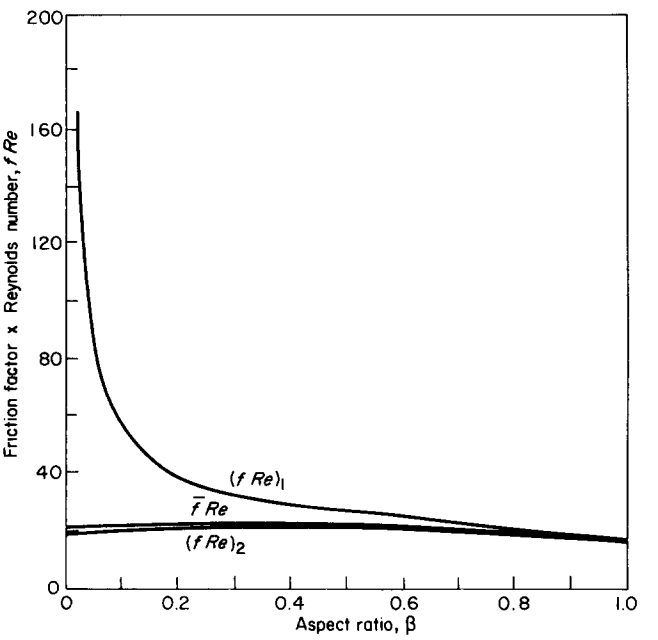

Fig 7 Friction factors for annuli with an equilateral triangular core. Number of elements is 145

Friction factors

The variations of $\bar{f}\,Re$ with aspect ratio have been reported by Cheng and Jamil[7] and by Hagan and Rathowsky[8]. The same trends as shown in Fig 8 were observed.

The results for $(f\,Re)_1$ and $(f\,Re)_2$ are expected to be useful in predicting the trends of the variation of Nusselt number for forced convective heat transfer in non-circular annuli, utilizing the analogy between the momentum and heat transfer processes, ie Reynolds' analogy. This is discussed in an accompanying paper on heat transfer through such passages[15].

Validity of the use of the hydraulic diameter

The validity of the use of the hydraulic diameter D_h as a characteristic length for non-circular annuli is examined. Though the hydraulic diameter is used in the evaluation of Reynolds number and $\bar{f}\,Re$, it is observed that $\bar{f}\,Re$ values depend on the geometry of the annulus and that these values deviate significantly from those for a circular annulus or from that for the circular tube. Of course, $\bar{f}\,Re$ values for the non-circular annuli with an 18-sided core almost coincide with those for a circular annulus for the range of aspect ratio from 0.02 to 0.9. Thus, in most cases the use of the hydraulic diameter does not yield a single relation for all the annuli studied; the sharper the corner of the core, the more is the deviation from the circular annulus case.

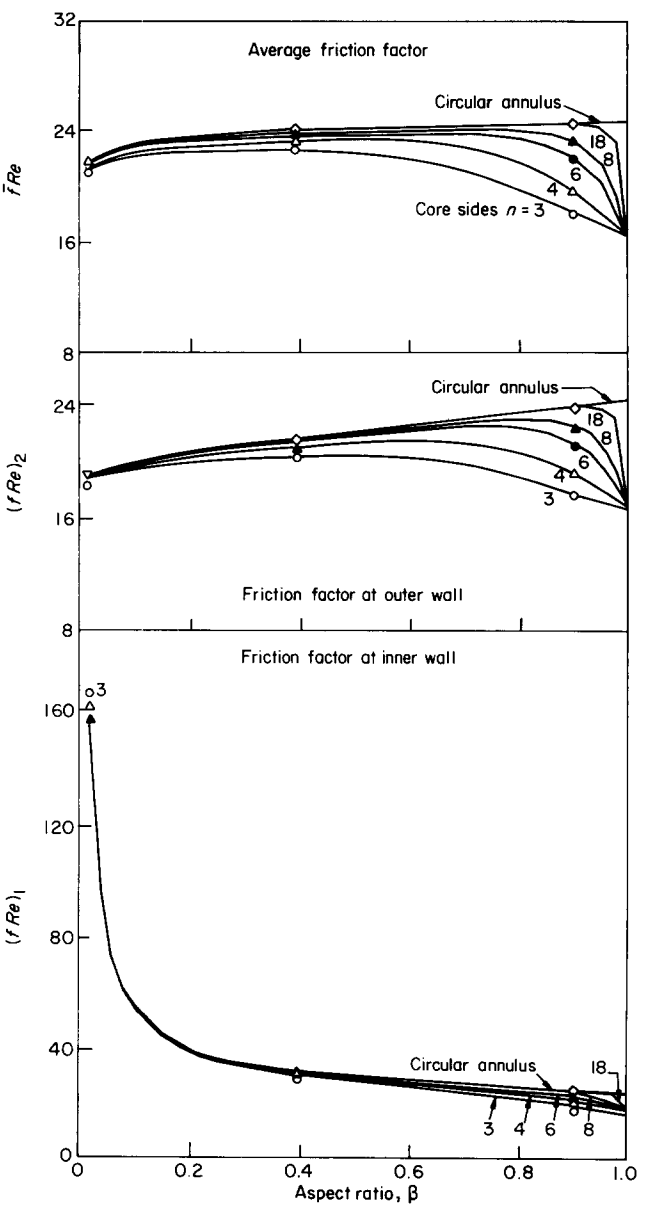

Fig 8 Friction factors for various annuli studied

Table 2 Constants in $\bar{f}$ Re correlation (cubic form of Eq (3)) for aspect ratio range of 0.1 to 0.9

Number of core sides	a_1	b_1	c_1	d_1	Stand. dev.
3	21.4858	4.7089	−1.2317	−9.4801	0.001
4	22.3384	−0.9912	15.8175	−19.9758	0.004
6	22.5653	−0.0193	11.8938	−13.9276	0.006
8	22.3602	3.5026	1.7217	−5.1489	0.004
18	22.0220	8.4363	−11.5402	5.3467	0.001
Circular annulus (FEM)	21.8251	9.3210	−13.1759	6.3515	0.001

Overall correlations

An attempt is made to relate $\bar{f}Re$ to the aspect ratio so that by knowing just the aspect ratio one can predict fRe for the annuli under consideration. Correlations are obtained by the least square curve-fit method employing a polynomial equation in β of the form

$$\bar{f}Re = a_1 + b_1\beta + c_1\beta^2 + d_1\beta^3 + \ldots \quad (3)$$

The order of the polynomial is varied from one to seven. It is found that the higher the order of the equation, the better is the fit. But for simplicity, the lowest order equation which has reasonably low standard deviation is considered. A cubic equation is found suitable. The values of the constraints a_1, b_1, c_1 and d_1 for each annuli studied are given in Table 2.

Conclusions

For the flow field in the doubly connected duct geometries studied, and for the solution technique used, the following conclusions can be drawn.

(1) The present finite element algorithm successfully tackles the doubly connected ducts studied. Negative values of velocity and shear stresses, as encountered in the collocation methods[5], were not experienced with the present method.

(2) The velocity field can be described by the radial coordinate alone in the fully developed region up to a certain aspect ratio dependent on the shape of the inner core (Table 1).

(3) The resistance to fluid flow is predominantly high in the region close to the inner wall.

(4) In the corner region the shear stresses are significantly high.

(5) The hydraulic diameter D_h is not an adequate geometric parameter to account for the effect of the geometries investigated.

(6) The average friction factor has been expressed as a simple function of aspect ratio (Eq (3)).

(7) The average friction factors for the non-circular annuli studied are found to be less than that for a circular annulus for the same aspect ratio. Also, the friction factors for the non-circular ducts (eg for an equilateral triangular duct $\bar{f}Re = 13.33$; for a square duct $\bar{f}Re = 14.2$) are less than that for a circular tube ($\bar{f}Re = 16$). Hence, where mechanical power consumption is an important consideration in the design of heat exchangers, the application of the non-circular ducts and annuli is advantageous.

Acknowledgement

The financial support of BRNS, Department of Atomic Energy, Government of India is gratefully acknowledged.

The authors wish to record their thanks to Dr M. Malik, Reader in Mechanical and Industrial Engineering, University of Roorkee for his help in developing the finite element solution algorithm.

References

1. **Kays W. M. and London A. L.** *Compact Heat Exchangers, 2nd edn, McGraw Hill, New York, 1964*
2. **Shah R. K. and London A. L.** Laminar flow forced convection in ducts in *Advances in Heat Transfer, Supplement 1, Academic Press, New York, 1978*
3. **Boyd R. D.** A unified theory for calculating steady laminar natural convective heat transfer data for horizontal annuli. *Int. J. Heat Mass Transfer, 1981*, **24**(9), *1545–1548*
4. **Boyd R. D.** Experimental study of the steady natural convection in a horizontal annulus with irregular boundaries. *Natural convection in Enclosures, ASME HTD 19th National Heat Transfer Conference, Orlando, FL, 1980*, **8**, *89–95*
5. **Sastry U. A.** Heat transfer by laminar forced convection in multiply-connected regions. *Acta Technika, Hung., 1965*, **51**, *181–192*
6. **Solanki S. C., Krishna Murthy M. V. and Ramachandran A.** An analysis of flow through non circular annular passages. *Proceedings, 3rd National Conference on Fluid Mechanics and Fluid Power, IIT Kharagpur, 1972*
7. **Cheng K. C. and Jamil M.** Laminar flow and heat transfer in circular ducts with diametrically opposite flat sides and ducts of multiply connected cross sections. *Can. J. Chem. Eng., 1970*, **48**, *333–334*
8. **Hagan S. L. and Rathowsky D. A.** Laminar flow in cylindrical ducts having regular polygonal shaped cores. *Can. J. Chem. Eng., 1968*, **46**, *387–388*
9. **Rieger H. and Projahn U.** Laminar natural connection heat transfer in a horizontal gap bounded by an elliptic and a circular cylinder. *Numerical Methods in Thermal Problems, eds R. W. Lewis, K. Morgan and B. A. Schneflar, Pineridge Press, Swansea, UK, 1981*, **2**, *1039–1047*
10. **Banodekar R. W. and Date A. W.** Finite difference procedure for solution of Poisson equation over complex domains with Neumann boundary conditions. *Computer and Fluids, 1978*, **6**
11. **Solanki S. C., Krishna Murthy M. V. and Ramachandran A.** Flow through non-circular passages. *Paper No. 79-FE-12, Joint ASME/CSME Fluids Engineering Conference, Niagara Falls, NY, June 1979*
12. **Solanki S. C., Saini J. S. and Gupta C. P.** An experimental investigation of fully developed laminar flow in a non circular annulus. *8th National Conference on Heat and Mass Transfer, Visakhapatnam, 1985, A 34-HMT-85*
13. **Huebner K. H.** *The Finite Element Method for Engineers, John Wiley, New York, 1975*
14. **Sparrow E. M. and Haji Sheikh A.** Flow and heat transfer in ducts of arbitrary shape with arbitrary thermal boundary conditions. *Trans ASME, J. Heat Transfer, Nov 1966, 351–358*
15. **Solanki S. C., Prakash S., Saini J. S. and Gupta C. P.** Forced convection heat transfer in doubly connected ducts. Submitted to *Int. J. Heat and Fluid Flow*